UCRL-JC-113782
PREPRINT

Validation of a Procedure for Calculating Broadband Strong Motion Time Histories with Empirical Green's Functions

S.P. Jarpe
P.W. Kasameyer

This paper has been accepted by
The Bulletin of the Seismological Society of America

February 1996

UCRL-JC-113782
Preprint

Validation of a Procedure for Calculating Broadband Strong Motion Time Histories with Empirical Green's Functions

S. P. Jarpe
P. W. Kasameyer

This paper has been accepted by

The Bulletin of the
Seismological Society of America

February, 1996

Validation of a Procedure for Calculating Broadband Strong Motion Time Histories with Empirical Green's Functions

S. P. Jarpe
P. W. Kasameyer

Lawrence Livermore National Laboratory

Abstract

We quantitatively evaluate the validity of an approach to calculating strong ground motion time histories that involves the kinematic modeling of earthquake rupture by using recorded empirical Green's functions to constrain the propagation path and site contribution in the period range 0.05 to 2.0 seconds, leaving only the contribution of the source to be specified. In addition, we use numerical Green's functions for long periods (> 10 seconds) where the average crustal structure is assumed to be well known. In the intermediate band (2 to 10 seconds) where site and path effects are still important, but empirical Green's functions have small signal-to-noise ratios, we use an arbitrary smoothing method to connect the numerical and empirical Green's function synthetics. The evaluation presented here consists of comparing actual recordings of the Loma Prieta earthquake at 26 sites to syntheses from a simple source model similar to what is thought to have occurred during the Loma Prieta earthquake. We show that the standard error between observed and predicted response spectra is less than or equal to errors from other methods for periods between 0.05 and 0.4 sec, and is significantly less than regression methods based on pre- Loma Prieta empirical strong motion data at periods between 0.5 and 5.0 sec.

The strong ground motion prediction methodology that we are validating provides an accurate, defendable means to characterize site and path effects, and therefore allows the uncertainties in the predicted hazard to be due to unresolved issues about the earthquake source such as the geological constraints of a particular fault and details about the physics of earthquakes. This methodology produces accurate and realistic acceleration and displacement time histories, which are becoming increasingly important for modeling the nonlinear response of large, distributed structures and soft soils. The implication for strong ground motion prediction is that a range of representations of an earthquake source based on physically realistic parameters can be used to generate a suite of possible time histories that represent the range of ground motion for that specific site and earthquake. In addition, in the future, as more information about a particular fault and earthquakes in general becomes available, the uncertainty in ground motion prediction should decrease.

Introduction

The rapidly developing sophistication of dynamic soil and structural analyses that include nonlinear effects (i. e., McCallen and Romstad, 1994, McCallen and Hutchings, 1995) require ground motion time histories rather than spectra as input. This paper evaluates a computational technique that provides full wavetrain, broadband, three-component, time histories resulting from extended rupture earthquakes (Hutchings and Wu, 1990; Hutchings 1991; Hutchings et al., 1992). This technique potentially could be used to compute ground motion estimates for all possible earthquake scenarios; however, in this paper we examine only the accuracy of the method when the extended rupture source is known. As a very simple but physically accurate description of the source is used, with only six free parameters, use of the method to produce time histories for a range of possible source models is practical. We examine quantitatively how well this methodology estimates the standard engineering parameters of peak acceleration, spectral response, and duration. We also show qualitatively how well actual time histories are replicated, recognizing that there is currently no widely accepted procedure for comparing observed and synthesized time histories for the purpose of assessing their effects on engineered structures.

There are many methods for computing earthquake ground motion parameters once a source has been identified. Generally, these methods can be described as one of either regression, stochastic, empirical, or quantitative methods. Regression methods predict parameters based on previously recorded ground motion, usually spectral response values and peak acceleration (Schnabel and Seed, 1973; Trifunac and Brady, 1975a; Joyner and Boore, 1981). Stochastic methods predict these parameters based on random vibration theory (Hanks and McGuire, 1981; Boore, 1983). Empirical time history methods use previously recorded strong ground motion time histories to represent the hazard under similar conditions (Bolt, 1992). Quantitative methods (including the approach examined here) attempt to calculate the ground motion directly (Archuleta and Day, 1980; Wald et al., 1988; Hutchings, 1991).

In this paper, we show that a quantitative method can be used to calculate ground motion time histories, and that it is as accurate as other methods in calculating engineering parameters when basic information about the source is known. The computational approach tested here models large earthquakes by solving the representation relation for a finite earthquake rupture. In this solution we discretize a potential fault rupture surface and appropriately sum point source Green's functions that are convolved with slip functions. This is the Green's function summation approach (Heaton, 1982). Hutchings and Wu (1990) have developed an exact solution to the representation relation that utilizes either empirical or synthetic Green's functions. Here, we use recordings of small earthquakes to provide empirical Green's functions for frequencies 0.5 to 33 Hz, and analytical calculations to provide synthetic Green's functions for frequencies 0.05 to 0.5 Hz. Empirical Green's functions are defined here as recordings of effectively impulsive point source events. There are several advantages to this approach: 1) it allows for a means to incorporate the variability of the potential rupture process while constraining path and site response, 2) it provides a means to make synthetic ground motions site specific as well as broadband, and 3) it computes the representation explicitly and is consistent with theoretical models of earthquake rupture. We will refer to this ground motion synthesis methodology as the "quantitative source, empirical path and site-broadband" (QSEPS-B) method.

Site-specific ground-motion computations are critical for accurate estimation of earthquake hazard. Many studies have shown that ground motion varies significantly between recording sites with similar geologic classifications (i.e., soil, rock), even those located close to one another. For example, during the Loma Prieta earthquake, peak accelerations at rock sites in San Francisco varied by a factor of 8 (Boore et al., 1989). Much of this variation was due to differences in the geology just beneath the recording sites, but some may be caused by features along the propagation path. In our approach, we use actual seismograms of small earthquakes at the site where the synthesis is generated. These recorded Green's functions include the response of the entire geologic structure from the fault zone to the recording site. Since very small earthquakes are used ($M < 3.0$), the appropriate number of small events usually can be recorded in a fairly short time period in a seismically active area.

Other approaches use actual recordings of earthquakes in the synthesis, but many do not take advantage of site specific information. Bolt (1992) uses the empirical time history approach; a strong motion recording from a similar size earthquake with similar recording geometry and geology is modified and used for a particular situation. This cannot capture the variability in the source rupture processes or site specific effects from propagation path or site geology. Wald et al. (1988) and Somerville (1993) use a moderate size earthquake and calculated Green's functions in a semiquantitative approach to calculate strong ground motion. Zeng et al. (1994) use a completely synthetic approach with a synthetic composite source model and calculated Green's functions. These approaches also cannot capture site-specific effects, but can model source variability. Approaches that use geotechnical information from the actual site can overcome some site-specific limitation, but uncertainties that are due to site geology can still be large (Wong et al., 1993), Cramer et al. (1995). Field and Jacob (1993) and Cramer et al. (1995) conclude that actual earthquake recordings provide better constraints on site response than modeling based on geotechnical data.

We model the rupture process as a continuous rupture over the fault with smoothly varying slip amplitude that can result in one or more areas of high slip. This model of rupture is consistent with inversion results of slip distribution from past earthquakes (Wald et. al., 1990, 1993, 1995; Beroza and Spudich, 1988; Hartzell and Heaton, 1988; Hartzell 1989). This source model is different than is commonly used by most methodologies that utilize empirical Green's functions, which have a multitude of small events rupturing independently over the fault surface (Irikura, 1983; Papageorgiou and Aki, 1983; Munguia and Brune, 1984; Joyner and Boore, 1986; Boatwright, 1988; Wennerberg, 1990; and, Aki and Irikura, 1991). Composite models of faulting rely on scaling relations of earthquakes to determine the number of small earthquakes necessary to synthesize a large earthquake, and have a difficulty in matching the low and high frequency of synthesized seismograms to observed records (Joyner and Boore, 1986; Boatwright, 1988; Frankel 1995). Our modeling approach only requires that the number of small earthquakes used in the synthesis is such that the sum of their moments add up to the moment of the large earthquake, which matches the low frequency of observed seismograms. The high frequency is matched simply by using appropriate rupture parameters (Hutchings, 1994).

This method is consistent, within the frequency range of resolution of inversion studies, with what is known about how earthquakes rupture. However, inversion studies only resolve fault slip histories up to spatial resolution of a couple of kilometers and frequencies up to one hertz. Nevertheless, this method provides good fits to observed seismograms up to 25 Hz when these models are used. It is true that there is little or no information about what the faulting process is for shorter wavelengths or higher frequencies. However, the complexity added to rupture by composite earthquake models or by highly variable rupture models is not necessary to synthesize observed seismograms, and there is no evidence that earthquake rupture is highly complex at short spatial or temporal dimensions.

Hutchings (1991) demonstrated the empirical Green's function method of Hutchings and Wu (1990) by "predicting" actual recorded ground motion from the Loma Prieta earthquake at 5 Bay Area sites using recordings of Loma Prieta aftershocks. He presented 25 source models that in his estimation spanned the uncertainty in the source prior to the occurrence of the Loma Prieta earthquake. Hutchings (1994) also compared time series and spectra derived from the same method to actual strong motion recordings of the San Fernando earthquake at three sites; however, neither of these studies rigorously validated the approach with a large number of observed strong motion recordings.

In this paper, we extend the synthesis approach of Hutchings and Wu (1990) to cover a broader band, and evaluate the method by presenting the results of syntheses from Hutchings' (1991) 5 sites and 21 additional sites where both the Loma Prieta main shock and aftershocks were recorded, including the strong motion sites nearest the fault. These syntheses use a very simple, generalized rupture model based on independent studies of the Loma Prieta earthquake. Because Hutchings' approach uses small earthquakes whose low-frequency energy is less than the background noise, and is therefore limited to frequencies above 0.5 Hz. We propose an extension, the QSEPS-B method, to extend to frequencies below 0.5 Hz by merging strong motion syntheses derived from synthetic Green's functions with the empirically based syntheses. We note that because the synthesis approach is based on site response from very small ground motion, it is only valid for linear material response. We will present evidence that some soft soil sites responded nonlinearly, but for this earthquake the linear predictions do a surprisingly good job of fitting engineering parameters at the soft soil sites as well.

We compare the synthesized ground motion to the observed ground motion at each site in three ways. 1) We qualitatively compare the synthetics to the observations in terms of their acceleration and velocity time series and response spectra. Although such a qualitative comparison of time histories is inexact and not a rigorous validation of the calculation procedure, we do it because the most important contribution of this method is to provide realistic time histories that can be used in structural calculations that require time history input. 2) We estimate prediction errors for several engineering parameters (especially response spectral ordinates) by comparing observed and calculated parameters. These errors are shown to be equal to or smaller than error estimates from other strong motion calculation methods, particularly at periods between 0.5 and 5.0 sec. 3) Recognizing that the prediction of *time histories* as well as spectra are important, we develop a simple, quantitative scheme based on the response spectrum to capture the time history character of a seismogram and show that our synthesized time histories match the observed records using this scheme.

Sites and Seismic Recordings

Table 1 summarizes information about the sites we analyzed. Main shock recordings were provided by the USGS (Maley et al., 1989) CSMIP (Shakal et al., 1989) and LLNL (Jarpe et al., 1989). Aftershock recordings were provided by the USGS (Mueller and Glassmoyer, 1990), and (Carver et al., 1990), and LLNL (Jarpe et al., 1989). The stations BEC, FSC, MSJ, CEG, and YBI are the five sites studied by Hutchings (1991). Figure 1 shows the locations of the stations and the approximate source region of the Loma Prieta earthquake.

All weak motion data were instrument corrected to have a flat response to velocity between 0.5 and 25 Hz. Strong motion data were processed by the distributing organizations with different long-period cutoff frequencies for each station. We have used only data from the valid band of the observed records when comparing synthesized and observed data at a particular station. Hypocentral locations and local duration magnitudes of the empirical Green's functions were obtained from USGS (1990). The site geology classifications are from Boore et al. (1993). Table 1 indicates how many empirical Green's functions were used in the syntheses at each station and the magnitude of the largest empirical Green's function.

Strong Motion Synthetic Seismogram Calculation Procedure

The strong motion syntheses were performed by the empirical Green's function method described by Hutchings and Wu (1990) and Hutchings (1991). It utilizes empirical and synthetic Green's functions along with a kinematic description of fault rupture to synthesize seismograms. The method avoids the common approximation made in summing empirical Green's functions that the large event is the sum of several moderate events, and many of the problems associated with deciding how those events should be summed (see Hutchings (1994). In this method, the only parameters required to characterize a particular earthquake source are moment, fault orientation, fault area and shape, slip vector, hypocenter, and rupture velocity. In order to avoid circularity, we have determined values for these parameters from independent studies of the Loma Prieta earthquake that use teleseismic and regional seismic recordings and geodetic data, avoiding the use of information derived from the strong motion data we are using for this evaluation.

The Loma Prieta source is modeled as a two-dimensional elliptical rupture, initiating at the

TABLE 1

sta	lat(N)	lon(W)	site geology	strong motion station	weak motion data	distance	#EGF	max mag.
HAL	37.338	121.714	B	CSMIP_57191	USGS[1]	—	5	3.2
KOI	37.0462	121.8031	B	CSMIP_57007	USGS[1]	—	36	2.8
RIN	37.786	122.3907	A	CSMIP_58151	USGS[1]	25 m	5	3.9
CAP	36.9740	121.9522	B	CSMIP_47125	USGS[1]	—	14	2.5
CAL	37.7899	122.4287	A	CSMIP_58131	USGS[1]	—	7	4.0
DIA	37.7400	122.4330	A	CSMIP_58130	USGS[1]	—	5	3.4
ASH	37.3986	121.9514	C	CSMIP_57066	USGS[1]	90 m	3	2.8
AP7	37.485	122.3132	B	CSMIP_58378	USGS[1]	—	5	2.6
GA2	36.973	121.568	B	CSMIP_47006	USGS[1]	—	6	2.8
MON	36.5970	121.8969	A	CSMIP_47377	USGS[1]	—	6	2.7
SAR	37.2553	122.0311	B	CSMIP_58065	USGS[1]	—	22	2.7
RAV	37.490	122.125	soft soil	CSMIP_58596	USGS[1]	1000 m	5	3.2
DMD	37.1642	121.6314	B	USGS_1652	USGS[1]	—	31	2.9
SAG	36.764	121.446	A	USGS_1032	USGS[1]	—	6	3.0
EMT	37.844	122.295	soft soil	USGS_1662	USGS[1]	?	1	3.7
SF1	37.622	122.398	C	CSMIP 58223	USGS[1]	—	1	3.8
POR	37.535	121.929	C	USGS_1686	USGS[1]	—	7	3.6
LOE	37.0005	122.0562	B	CSMIP_58135	USGS[2]	—	8	3.2
MSJ	37.530	121.9190	B	CSMIP_57064	LLNL	—	3	3.7
FSC	37.544	122.232	soft soil	CSMIP_58375	LLNL	50 m	5	3.7
YBI	37.808	122.360	A	CSMIP_58163	LLNL	—	12	3.7
TRI	37.825	122.370	soft soil	CSMIP_58117	LLNL	—	5	3.7
BEC	37.795	122.395	soft soil	Bechtel Corp.	LLNL	10 m	2	3.3
CEG	37.687	121.701	C	LLNL	LLNL	—	6	3.1
CPP	37.7017	121.6835	B	LLNL	LLNL	—	7	3.7
CSA	37.6738	121.7042	B	LLNL	LLNL	—	7	3.7

USGS[1]: Mueller and Glassmoyer (1990).
USGS[2]: Carver et al., (1990).
LLNL: Jarpe et al., (1989).
distance is distance between weak motion and strong motion sensor locations.
#EGFs is the number of empirical Green's functions used in the EGF synthesis for that station.
Max. mag. is the local magnitude of the largest EGF used in the synthesis for that station.

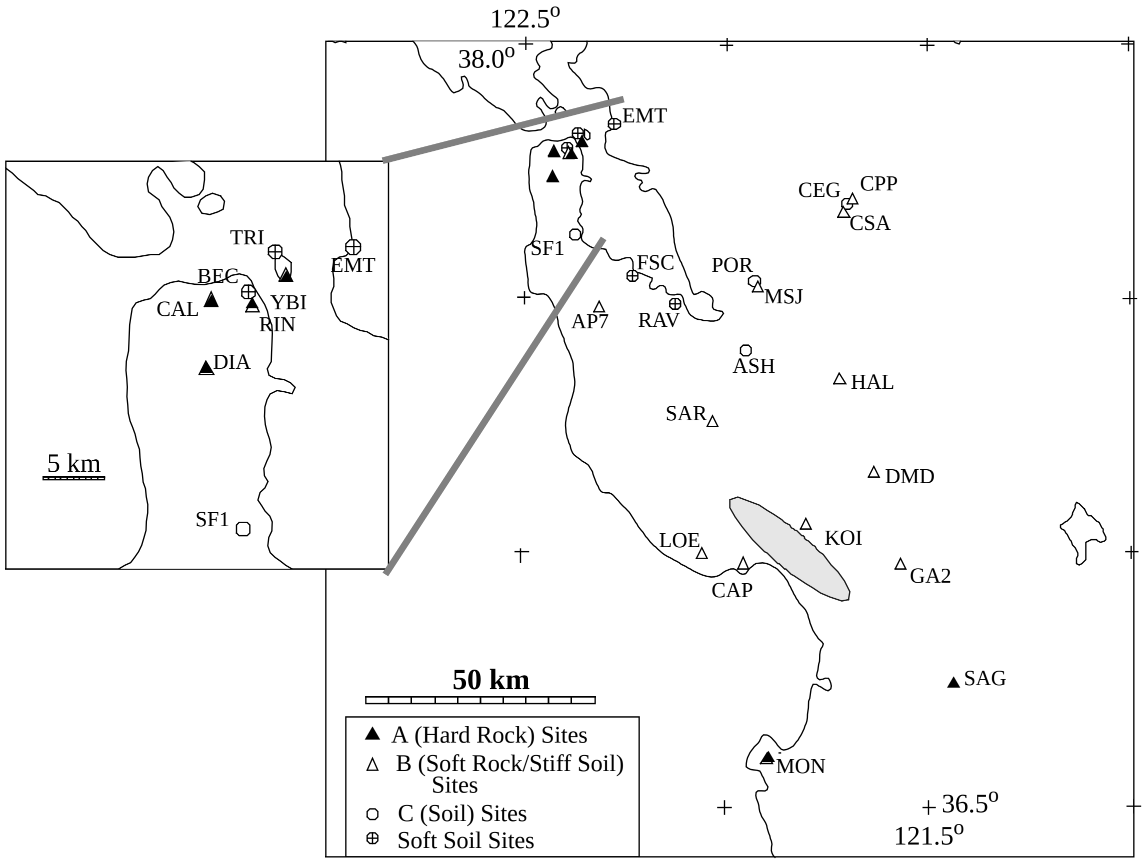

Figure 1. Locations of the sites used in this study, and the surface projection of the source region of the Loma Prieta earthquake, designated by the ellipse. The triangles represent rock sites and the circles are soil sites. Soft soil sites are designated by crossed circles. The inset shows the sites in and near San Francisco.

hypocenter and propagating radially at the specified rupture velocity (Figure 2). This simple model obviously ignores many of the complexities that occur on the rupture surface; however, it represents the level of knowledge that we could appropriately use when predicting future strong ground motion. The main purpose of this paper is to compare syntheses from a relatively simple model to real strong motion observations, so that we can assess the uncertainties that arise from the QSEPS-B calculation procedure itself, independent of uncertainties due to incomplete knowledge about future earthquakes.

The source model we used for the evaluation of the synthesis method will be referred to as the Loma Prieta model. We calculated one realization of this source model for each recording station. This model has approximately the same fault plane (area, spatial location, and shape) moment, rupture-time history (bilateral rupture), and peak displacement as have been determined independently from the modeling of teleseismic, regional seismic, and geodetic data [Hartzell et al. (1991), Wallace et al. (1991), Snay et al. (1991)]. This model uses a Kostrov slip function (summarized in Hutchings, 1991 and Hutchings, 1994). The EGF strong motion syntheses were performed as described in Hutchings (1991) and Hutchings (1994), except that focal mechanism corrections were not performed.

As Hutchings (1991) observed, the empirical Green's functions do not have energy above the noise level below 0.5 Hz, but the effective bandwidth of the synthetic strong ground motion can be increased by combining it with strong motion time histories derived from numerical Green's functions (Hutchings et al., 1992). To accomplish this, additional strong motion syntheses were performed with numerical Green's functions calculated with a reflectivity method (Kennet, 1983) and the one-dimensional velocity model of Dietz and Ellsworth (1990). We used the same strong ground motion synthesis procedure as was used with the empirical Green's functions, except that focal mechanism corrections were made. The two resulting syntheses for each station were combined by merging the two waveforms using the procedure outlined below.

Because the amplitudes of numerical and empirical Green's functions do not usually match at 0.5 Hz, the lowest useful frequency band of the empirical Green's functions (for reasons discussed below), we employ a merging procedure that scales the amplitude of the numerical Green's function synthesis to match the empirical Green's function synthesis at 0.5 Hz. We assume that the one-dimensional velocity model produces the correct Green's functions at frequencies less than 0.1 Hz. The mismatch, which is often a factor greater than 5 at 0.5 Hz, indicates that near-surface and lateral effects are still present in the seismograms at frequencies between 0.5 and 0.1 Hz. In the absence of valid empirical data and detailed structural models in this frequency band, we arbitrarily modify the numerical time histories so they match the empirically-based time histories at 0.5 Hz. In the frequency domain, we multiply the time history by a smoothly varying function that equals one below 0.1 Hz and that makes the numerical synthesis match the empirical synthesis at 0.5 Hz. This process presumes that the numerical time histories have the correct moment at very long periods, and allows the extrapolation of the empirical information to lower frequencies (0.5-0.1 Hz). As will be shown below, this approach produces a good fit to the Loma Prieta observed data. Its general applicability must be tested with additional datasets.

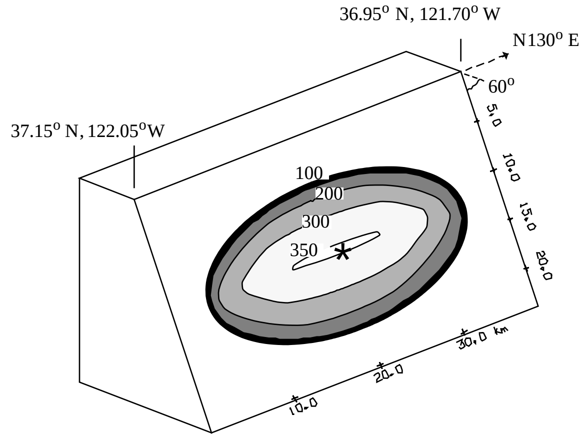

Figure 2. Fault model for the Loma Prieta earthquake that we use in this paper. The view direction is from the east and inclined 45°. Contours are slip in centimeters with a 100 cm contour interval. The hypocenter is shown by the asterisk. The moment of the Loma Prieta model is 3.0×10^{26} dyne-cm, the rupture velocity is 0.75 times the shear wave velocity, or approximately 2.6 km / sec. The strike is N130E and the dip is 60° to the NE. These input parameters result in a maximum displacement of 390 cm, and a stress drop of 85 bars.

Results of Syntheses with the Loma Prieta Source Model

Hutchings (1991) found that he could produce time series that "subjectively" agreed with observations at 4 of 5 sites, and he argued that his method captures much of the site-to-site variability, including amplitude and frequency content variations, and that it produces a general match to the shape of the response spectra. We find that his method and general source parameters determined by independent studies produce a similar agreement at most of our 26 sites. We will show several examples to illustrate the success and importance of this result, and then discuss the statistical measures of that success. In the examples, we compare the acceleration and displacement time series and the acceleration response spectra from the syntheses of the Loma Prieta model to the corresponding time series and spectra from recordings of the Loma Prieta earthquake. We will examine sites with unusually high and low peak acceleration values, a rock site close to the Loma Prieta earthquake where significant ground motion amplitudes (> 0.2 g) were observed, a rock site in San Francisco, where unexpectedly high peak accelerations were recorded, and finally, a soft soil site where nonlinear soil response is likely to have occurred.

Figure 3 illustrates the variations in amplitude that were seen for the Loma Prieta Earthquake, and the ability of QSEPS-B to capture them. The observed peak accelerations for the data set studied here show variations on the order of a factor of 6 at some distances. Figure 3 shows how well QSEPS-B, with a simple source model, can synthesize the time histories for stations near the extremes of this

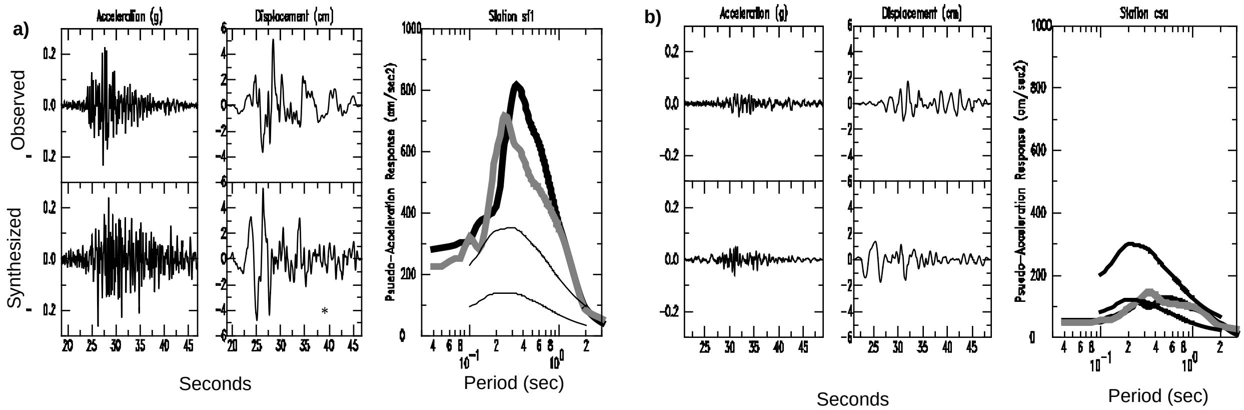

Figure 3. Motivation for the broadband EGF methodology. a) Comparison of synthesis and observations of the Loma Prieta earthquake at a soil site (site classification C) at the San Francisco Airport (SF1) 67 km from the rupture. c) Same for station CSA, a soil site (site classification B) at 68 km. At the left are the observed and synthesized acceleration time histories for one horizontal component, in the center are the corresponding displacement traces, and at the right are the pseudo-acceleration response spectra (observed-thick dark, synthesized- thick light). The response spectra were calculated at 15 periods and interpolated to produce the spectra shown. Also plotted are the ± 1 standard deviation bounds from the Boore et al.(1993) regression for pseudo-acceleration response (thin solid, labeled $\pm\sigma$, BJF93).

distribution. This figure illustrates that 1) the “simple” source model produces realistically complex acceleration and displacement seismograms with envelopes that generally match the observations; that 2) the synthesis approach replicates the peak acceleration and pseudo-acceleration response values that differ by factors of 4 to 8 at these two stations, and that 3) the relative hazard at these two sites could have been estimated without knowledge of the geology before a large earthquake occurred, assuming that empirical Green’s functions had been available.

In Figure 4, we compare the Loma Prieta model synthesis and observed time series and spectra at a rock site close to the center of the Loma Prieta rupture surface. The close agreement between the observed and synthesized time series and spectra at this station shows that the method can capture near-source, finite-fault effects as well as site variability at stations very near the rupture surface. By comparing Figures 3 and 4, we see that the synthesis approach captures variations in duration and in frequency content at different sites.

The method produced slightly less satisfactory results at two types of sites: soft soil sites where our linear assumptions are significantly violated, and, inexplicably, at three rock sites in and near San Francisco. In Figure 5, we show time series and spectra at one rock site in San Francisco, station CAL, at which our calculated time series and spectrum match the observed in general shape and peak amplitudes. At three other sites, RIN, YBI, and DIA, however, the calculated peak accelerations were approximately half the observed peak accelerations. The disagreement between observed and predicted results at these three sites remains a

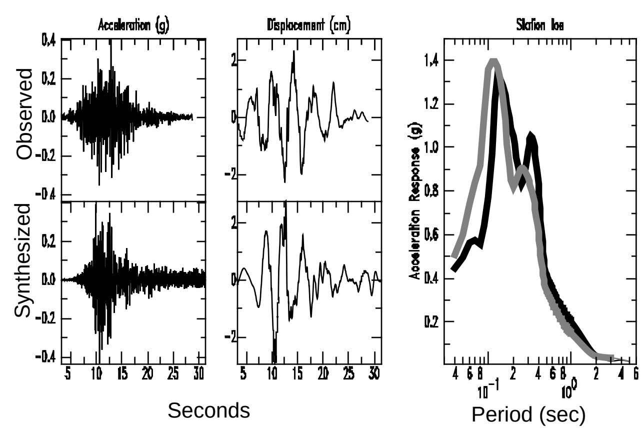

Figure 4. Comparison of time series and spectra from the preferred model synthesis and observed recordings of the Loma Prieta earthquake at a rock site (LOE, 10 km) close to the rupture. At the left are the observed and synthesized acceleration time histories for one horizontal component, in the center are the corresponding displacement traces, and at the right are the spectral acceleration response spectra (observed-solid, synthesized-light). The response spectra were calculated at 15 periods and interpolated to produce the spectra shown.

mystery to us, and to others using different methods [Boore et al., 1989, Linda Seekins, personal communication; Walt Silva, personal communication]. Somerville and Yoshimura (1990) propose that critical Moho reflections caused ground motion amplifications in San Francisco; QSEPS-B should include those effects because they should be present in the empirical and numerical Green's functions.

Figure 6 shows the spectra and time series for the Treasure Island (TRI) site, which is located on soft soil. Here, the early portion of the observed record is similar to the syntheses, but the recorded amplitudes die rapidly on the observed records. The nearly complete cessation of shaking at this time at TRI apparently reflects the dominance of strongly nonlinear effects (presumably liquefaction) in the near-surface soils (Darragh and Shakal, 1991; Jarpe et al., 1989), a phenomenon that is not accounted for in the QSEPS-B method. This effect is also evident, although not as strongly, in the comparison of the observed and synthesized records at the other soft soil sites FSC, RAV, BEC, and EMT, and even at station KOI, which is a stiff soil site very close to the rupture. To use QSEPS-B at a soft soil site, or a stiff soil site very close to the rupture, the synthesized motion must be used as input to a model that accounts for these nonlinear effects (i.e., Schnabel et al., 1972 or Popescu and Prevost, 1993).

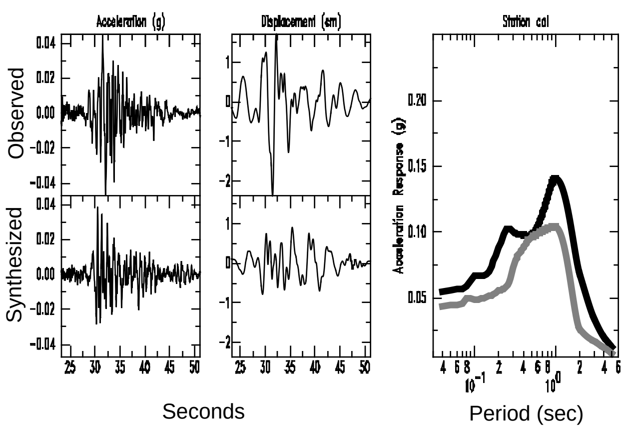

Figure 5. Time series and spectra from the Loma Prieta model synthesis and the Loma Prieta earthquake at a rock station (CAL, 95 km) located at the northern end of the San Francisco peninsula. For a detailed explanation, see the caption for Figure 4.

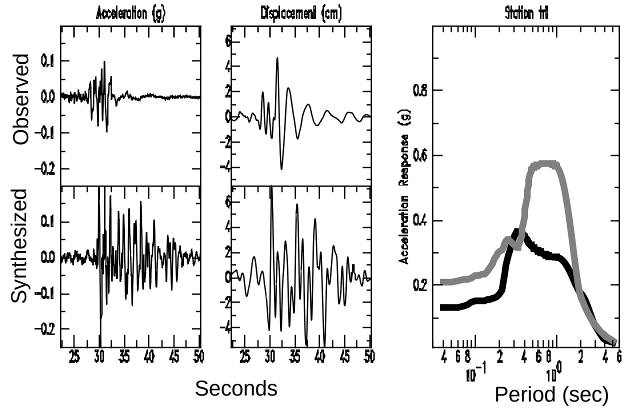

Figure 6. Time series and spectra from the Loma Prieta model synthesis and the Loma Prieta earthquake at a soft soil station (TRI, 98 km) where nonlinear soil behavior was observed. For a detailed explanation, see the caption for Figure 4.

Quantitative Evaluation of Modeling Approach

The subjective agreement of prediction and observation motivates us to quantitatively evaluate the QSEPS-B modeling approach and assess the uncertainties involved in predictions based on it. In doing this, we follow the work of Abrahamson, et al. (1990) (also see Somerville, 1993), who correctly recognized that quantitative estimates of uncertainty are needed to make numerical methods useful. They choose to quantify the goodness-of-fit between simulated and observed ground motions by examining how well the calculated standard engineering parameters match the observed data. We will present a brief summary of their analysis and use their framework to evaluate our Loma Prieta results.

Mathematical Framework

For one earthquake and the *j*th station, each engineering parameter, represented by p_j, is given by

$$ln(p_j^o) = ln(p_j^c) + \mu^p + \varepsilon_j^p,$$

where *o* and *c* refer to observed and calculated, and μ^p is the model bias for the parameter *p*. The ε_j^p are the errors in fitting the *j*th station and are assumed to be normally distributed, independent errors with zero mean and variance σ_ε^2.

Abrahamson, et al. 1990, recognized that the bias and errors arise from three sources: 1) modeling error caused by the approximations and incorrect assumptions in our method of calculation; 2) random error caused by the details of the source and propagation that cannot be measured or modeled deterministically; and 3) parametric uncertainty caused by uncertainty about the detailed characteristics of a particular future earthquake. They also point out that we cannot separate modeling and random uncertainty, so we can only estimate their combined effect, which we do in this section, ignoring parametric uncertainty.

Abrahamson et al. (1990) calculated engineering parameters for three earthquakes and used the above equation to estimate the standard deviation of the modeling error of the numerical calculations. We use our Loma Prieta model to calculate the modeling error for the QSEPS-B method, which we compare to uncertainties from several other methods.

For each parameter *p* the bias and standard error, *s*, can be estimated by fitting $ln\,(p_j^o)$ vs. $ln\,(p_j^c)$, assuming a slope of 1. Uncertainties in these estimates are calculated using standard formulae (e.g., Freund, 1962). The standard deviation of the bias estimate is approximated by the standard error divided by $\sqrt{n-1}$, and the 68% confidence interval of the variance is

$$(n-1)\frac{s^2}{\chi^2_{n-1,\,0.84}} < \sigma^2 < (n-1)\frac{s^2}{\chi^2_{n-1,\,0.16}},$$

where n is the number of observations, and $\chi^2_{n-1,\,\alpha}$ is the value of the chi-square distribution for n –1 degrees of freedom.

The standard engineering parameters that we use for validation are peak acceleration, duration, RMS acceleration, and acceleration response. Following Joyner and Boore (1981), we define peak acceleration to be the maximum of the two horizontal components. Duration is defined as the time interval between 5 and 75% of the integrated acceleration power of the entire record averaged over the two horizontal components. We use 75% instead of the original 95% defined by Trifunac and Brady (1975b) because Kennedy et al. (1984) found that small accelerations at the end of the record that don't contribute to damage increase the duration when the 95% threshold is used. RMS acceleration is defined as the square root of the total energy in the time interval described above divided by the duration (Kennedy et al., 1984). Absolute acceleration response is calculated for 5% damping and is averaged over the two horizontal components.

Figure 7 shows the individual data and results for the error calculations for the parameters peak acceleration, duration, RMS acceleration, and acceleration response at a 1.0-sec period. As discussed earlier, we note that the sites where the parameters derived from the syntheses differ from the observed parameters by more than a factor of 2 are three rock sites in San Francisco (YBI, RIN, and DIA), which have lower predicted peak and RMS acceleration values than observed. Even with these points included, our observed bias estimates are slightly greater than zero, except for the duration. Our linear calculations overpredict the durations at the soft soil sites, which is expected if those sites responded nonlinearly during the Loma Prieta earthquake. The calculated RMS accelerations at those sites (Figure 7c) match the observed values, which indicates that we also overpredict the energy. The poor correlation between the observed and calculated durations is mainly due to the small range spanned by the observed durations, which are largely controlled by the Loma Prieta source duration. An exception to this is the outlier in Figure 7b, which has a very short duration (> 3 sec) that we were able to correctly duplicate. A dataset containing records from several earthquakes of different source duration would be more suited to studying the fit between observed and predicted durations.

Comparison to Other Prediction Methodologies

We have assembled estimates of the modeling errors for three methods of predicting strong ground motion for comparison to the errors from our method. 1) Using the empirical relationships of Joyner and Boore (1988) and Boore et al., (1993), we have calculated the predicted peak acceleration and pseudo-velocity response (bias and standard errors are equivalent for pseudo-velocity response and absolute acceleration response) for a *M* 7.1 earthquake at each of our stations. For the Joyner and Boore (1988) calculations, we classified "A" and "B" sites as "rock" and "C" sites as "soil". 2) We have used 14 (post) predicted peak acceleration

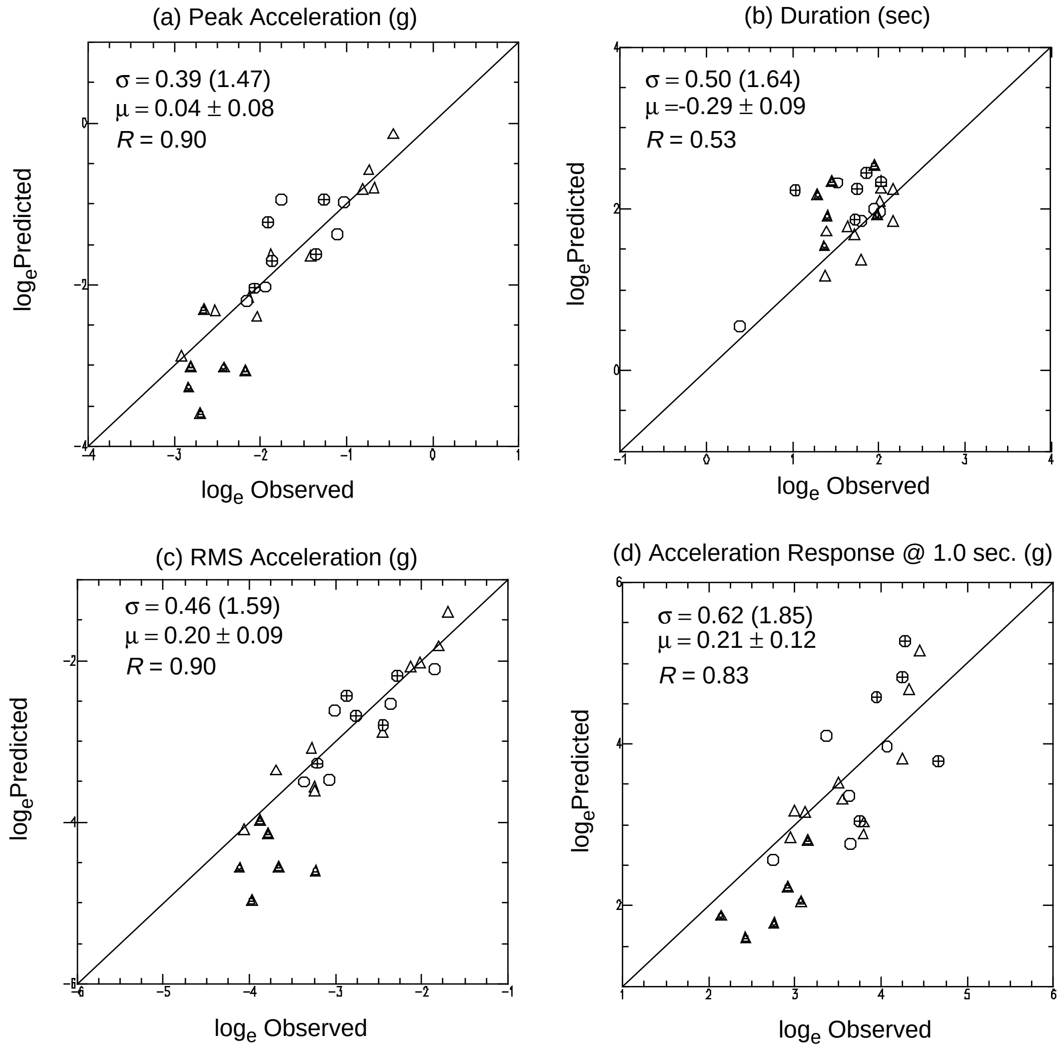

Figure 7. Comparison of engineering parameters observed for the Loma Prieta earthquake with those derived from the Loma Prieta model. The observed value is plotted on the horizontal axis, and the predicted value is on the vertical axis. The parameters shown are a) peak acceleration, b) duration, c) RMS acceleration, and d) acceleration response at 1.0-sec period. On each plot, a line with slope 1 represents a perfect fit between the calculated and observed values. The mean μ^p with its uncertainty (standard deviation) and standard deviation σ_ε of the differences between the observed and calculated values are shown for each parameter and are expressed as $\log_e$ and factors (in parenthesis). The correlation coefficient R is also shown for each parameter. The symbols signify the site type as in Figure 1.

values of Chin and Aki (1991) for the Loma Prieta earthquake derived from their numerical simulation. We only used their data from stations we used, and excluded soft soil sites. 3) We have used the modeling errors from Abrahamson et al. (1990), who compared their numerical peak accelerations and acceleration response spectra (calculated using the method of Wald et al., 1988) to observed values for three moderately sized earthquakes. We have included the errors determined by Anderson and Yu (1996) for the method of Zeng et al. (1994) for the Northridge earthquake. When comparing methods, we did not include soft soil sites because 1) the regressions of Joyner and Boore (1988) and Boore et al. (1993) did not include soft soil sites, and 2) because we do not claim to model the evident nonlinear behavior observed at these sites during the Loma Prieta earthquake.

Model Bias

We compare the bias (observed–predicted) for

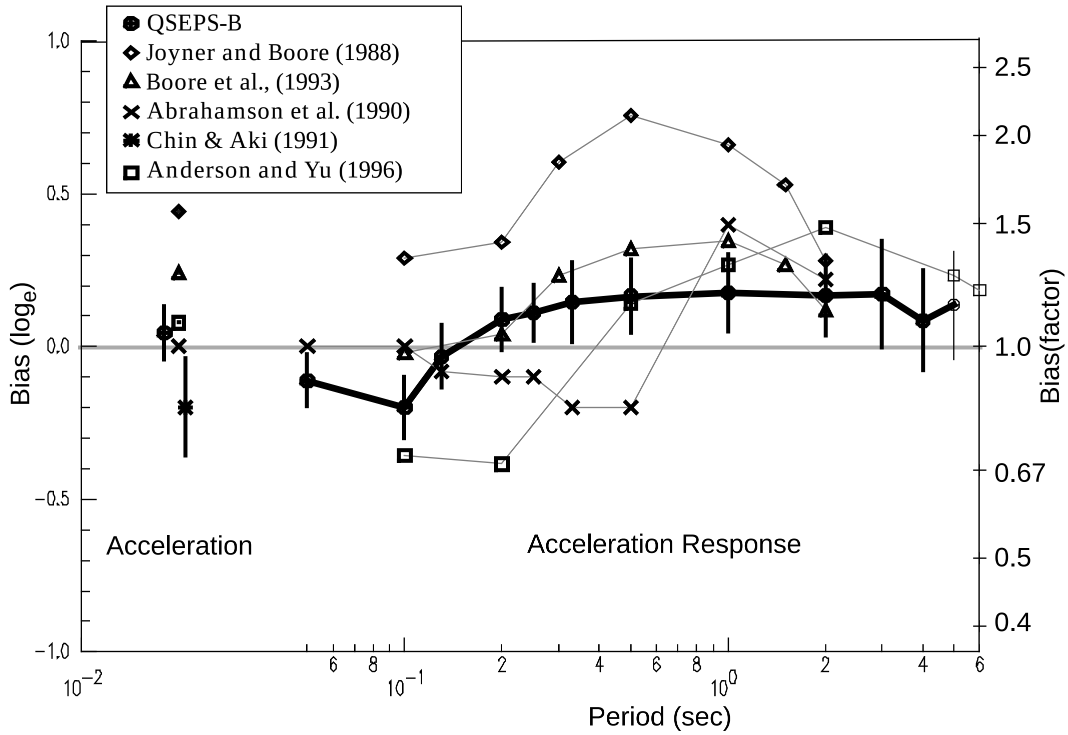

Figure 8. Model bias of calculated ground motion for several different ground motion prediction methods. Model bias is the average difference between the natural logs of observed and predicted parameters. The parameters shown are peak acceleration and acceleration response (Joyner and Boore and Boore et al. are pseudo-velocity response) at 5% damping. The different methods are described in the text. The uncertainty in the bias (standard deviation) for the broadband EGF synthesis is included. The uncertainties in the bias for the other methods are similar in size; they have been left off the plot for simplicity. The scale on the left is a $\log_e$ scale, and on the right the scale is bias expressed as a factor. The horizontal line is drawn at zero bias for reference.

the QSEPS-B Loma Prieta predictions to the bias of the other methods in Figure 8. The bias in peak acceleration is small (less than 0.1, or a factor of 1.1) for both the QSEPS-B results and the Abrahamson et al. study. For the Chin and Aki (1991) predictions, the bias is -0.24. They attribute this overprediction of peak acceleration to “pervasive nonlinear site effects” at rock and stiff soil sites, of which we see no evidence. For the empirical relationships of Joyner and Boore (1988), and Boore et al. (1993), the bias in peak acceleration and pseudo-velocity response at periods between 0.3 and 1.0 sec are significantly positive. A possible reason for the larger bias for the empirical relationships is that the three other methods used specific source information available after the earthquake(s) occurred, and the empirical methods use only limited source information (magnitude). Following Abrahamson, et al., we will assume that $\mu^p = 0$ when estimating the modeling uncertainty.

Modeling Plus Random Errors

The modeling plus random errors for peak acceleration and spectral response are shown in Figure 9. From these results, we conclude that, given the correct simple model for the earthquake source and linear site behavior, the QSEPS-B synthesis can produce estimates of engineering parameters that are as close to observed values as those of the other methods studied over a broad period range (0.04 to 5 sec).

This result is important for three reasons. First, we see no evidence of deficiencies in the spectra of the QSEPS-B synthesized records due to the effect of summing of small subevents (Joyner and Boore, 1986, 1988). Hutchings (1993) explains that this problem only occurs when the Haskell rupture model (which we did not use) is used. Second, QSEPS-B and Wald’s method do as well as the regression method of Boore et al. while not requiring an extensive database of strong motion data. These methods can be used in geographic areas

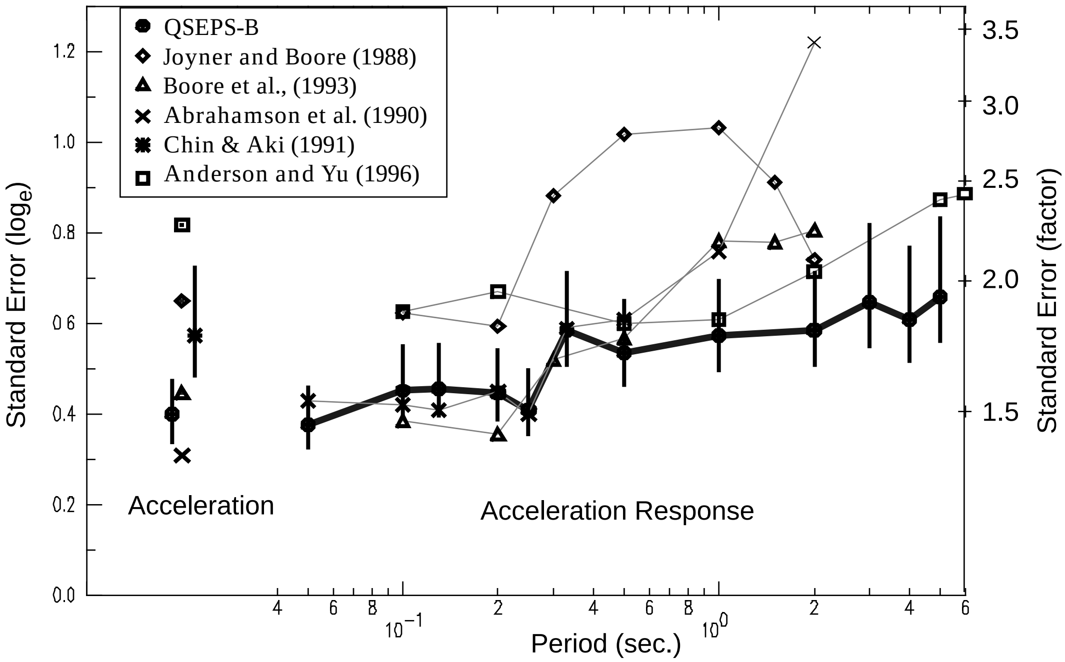

Figure 9. Calculations of random variation (modeling plus random error) of calculated ground motion for several different ground motion prediction methods. Standard error is the standard deviation of the difference between the calculated and observed parameter. The parameters shown are peak acceleration and acceleration response (Joyner and Boore and Boore et al. are pseudo-velocity response) at 5% damping. The different methods are described in the text. The scale on the left is a $\log_e$ scale, and on the right the scale is error expressed as a factor. Error bars, which represent the 68% confidence interval of the standard error, have been included for the broadband EGF synthesis. The uncertainties in the variance for the other methods are similar in size; they have been left off the plot for readability.

that lack strong motion data, and results derived from them will not be subject to modification after each major earthquake that adds to the strong motion database. Finally QSEPS-B does as well as Wald et al.'s method while not requiring either stochastic slip variation, gross information about the slip distribution derived from strong motion data, or information about site geology.

The last issue is illustrated by comparison with the work of Somerville (1993), who used Loma Prieta observed records for a similar validation of a strong motion prediction methodology using the method of Wald et al. (1988) of empirical source functions (strong motion recordings from earthquakes on other faults), a finite fault, and synthetic Green's functions. Using a complicated slip model on the fault and a one-dimensional regional propagation model with no local site- or path-specific information, Somerville reports model plus random errors similar to those we obtained with the QSEPS-B method, which ignores source complexity and accounts correctly for the station-specific site and path variations due to geologic complexities. The fact that methods dealing with different aspects of the hazard uncertainty perform similarly well raises an interesting question. The question of the relative contribution of source complexity versus site-and-path complexity to hazard estimate uncertainty needs to be analyzed further.

Sources of Modeling Plus Random Errors

The modeling plus random errors include: errors in the assumed rupture parameters such as rupture velocity, slip distribution, and rise times; nonlinear effects at the stiff soil sites; errors in the moments of the EGFs, and instrumental errors in the weak and strong ground motion recordings.

We accept the errors due to rupture parameters because we would like to show that the QSEPS-B method is not particularly sensitive to the choice of those parameters. We also accept the errors due to nonlinearity because at present, we have no proven way to correct syntheses derived from surface recordings for nonlinear site response at depth. We briefly address the two latter sources of error.

In the QSEPS-B method, the moments of the EGFs must be known. We used the relationship of Bakun (1984) to calculate moments for the EGFs from the duration magnitudes, and the error in the moment reported by Bakun (1984) is a factor of 1.6 (or $\log_e = 0.45$). If only one EGF were used in a synthesis, the error from just the moment uncertainty would approach our observed standard error for short periods. If we assume the errors for multiple EGFs are uncorrelated, the error due to the moment uncertainty would be proportional to $n^{-1/2}$ (n = number of EGFs), so that for 5 EGFs, the error contribution would be 0.20, and for 10 EGFs, it would be 0.14. We did not see a relationship between error and number of EGFs for this data set (for instance, only one EGF was used for station SF1; see Figure 3b).

Random instrumental errors in the recording of the EGFs should be small, but there could be systematic errors that we were unaware of (such as an incorrectly recorded gain factor or incorrectly calibrated sensor). We did our best to check for these errors, and could not find any evidence for them. Some of the observed strong motion records were not valid for periods greater than 2 sec due to the long period cutoff filters used in the processing, and we excluded them from the analysis for those periods. It is possible that there are significant long period errors in the observed data, which are obtained by digitizing analog film records. Iwan et al. (1985) found significant (as much as a factor of 10) long period errors for periods greater than 2 sec in one set of digitized, analog film, strong motion records by comparing it with data recorded by a colocated digital recorder.

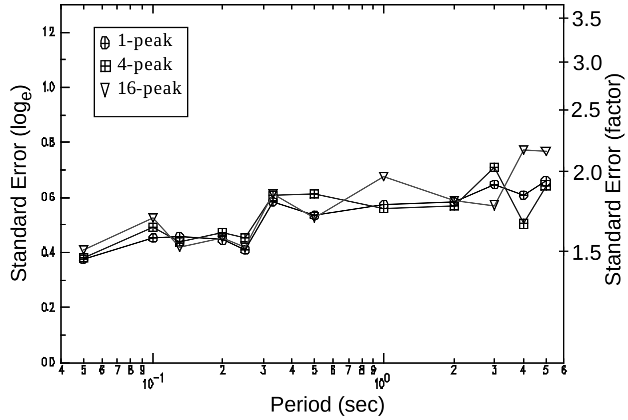

Figure 10. Calculations of random variation (modeling plus random error) of broadband EGF calculated ground motion for 1-, 4-, and 16-peak response spectra (defined in text). Standard error is the standard deviation of the difference between the calculated and observed acceleration response at 5% damping.

Goodness-of-Fit Parameters for Synthesized Time Histories

We have presented evidence that QSEPS-B Loma Prieta time histories "match" observed Loma Prieta time histories using several different engineering parameters. In addition to these properties, the empirical Green's function method produces realistic time histories, as we pointed out earlier. We do not expect a time history calculated from a simple source model to match each cycle of the observed signal. However, Hutchings (1991) contends that the time-histories we produce are useful for engineering purposes. We suggest additional measures to be used to quantify the goodness of fit of time series in a way that is useful in an engineering sense.

We propose a new method to evaluate the usefulness of calculated time histories. The basis for this measurement is the response spectrum; a calculated or predicted time history must first match the response spectrum of the observed or target time history. Two time series that have the same response spectrum can have very different character in the time domain; for example, all of the energy could occur with a relatively high amplitude in a very short time or be of lower amplitude and longer duration. The way we propose to embody this information is through the *n-peak response spectrum.* This concept is similar to one presented by Perez (1973). The traditional response spectral value at a given period T is the peak amplitude of the response of a single-degree-of-freedom damped oscillator with period T. The n-peak response spectrum is the amplitude of the nth highest peak in the same oscillator response. Therefore, the 1 peak response spectrum is the same as the traditional response spectrum, and the $n > 1$ peak response spectra have increasingly smaller amplitudes as n increases. The added information of the number of cycles at a given amplitude and period are useful for nonlinear structural damage models. To demonstrate that the *n*-peak response spectra of QSEPS-B Loma Prieta time histories match the observed n-peak response spectra as well as the traditional response spectra, we show in Figure 10 standard errors for 4- and 16-peak response spectra, in addition to the standard errors for the (1-peak) response spectra. These curves do not include soft soil sites.

Hazard Prediction

We have quantified the modeling and random error in ground motion predictions from the QSEPS-B method; these are errors that are due to factors that the method is unable to account for, such as insufficient number of empirical Green's functions to fully characterize the fault rupture surface, or insufficient or incorrect knowledge of the rupture parameters of the Loma Prieta earthquake. If we accept these errors, there still remains a potentially much greater source of error in a prediction of a future earthquake—parameter uncertainty. Parameter uncertainty arises from a very incomplete knowledge of the details of future earthquakes.

To estimate the uncertainty of a prediction of a future ground motion, we must identify the range of source parameters that could be possible for future earthquakes, and then assess their contribution to the residuals. The suitable range of possible source parameters is crucial to the assessment of prediction uncertainty, and different researchers make radically different assumptions about the range of potential rupture parameters. The resolution of these differences is of utmost importance for earthquake hazard estimation. Nevertheless, we contend that the QSEPS-B methodology that we are validating provides an accurate, defendable means to characterize site and path effects, and therefore allows the debate about source parameters to concentrate only on the geological constraints on a particular fault and some details about the physics of earthquakes in general that are still unresolved. For example, if a fault's moment, position, orientation, dominant motion (e.g., strike slip and reverse) and rupture surface are well known, then the uncertainty should be smaller than for a case where these parameters are poorly understood. Furthermore, after demonstrating that with accurate characterization of the site and path effects, useful engineering predictions can be made with relatively simple fault models. We expect that this method should lead to smaller parametric uncertainty than for methods that do not account for these effects. In addition, the parameter uncertainty should decrease with time as more is learned about particular faults and earthquakes in general. This new information can be immediately and easily incorporated into hazard predictions from this method because this method arises directly from accurate physical models of earthquakes, rather than from idealized, nonphysical representations of the earthquake source.

Conclusions

We have attempted to validate a ground motion synthesis procedure that incorporates 1) a faulting model that is physically consistent with what is known about the long-wavelength (> 1 km) behavior of earthquakes, 2) recorded empirical Green's functions that are small earthquakes on the fault of interest, and 3) calculated Green's functions to extend the synthesis bandwidth to very long periods. This validation consisted of showing qualitatively that the method can produce strong ground motion time histories that match observed time series and showing quantitatively that these time histories produce engineering parameters with errors smaller than or equal to those of other methods for the Loma Prieta earthquake. To validate this methodology, we produced broadband syntheses of the Loma Prieta earthquake at 26 sites at a range of distances from the fault, and we compared these syntheses to observed recordings. We showed that, using a relatively simple representation of the Loma Prieta earthquake that includes only moment, fault orientation, slip direction, hypocenter location, fault area, and rupture velocity, we reproduce the variations in observed strong motion due to source, path, station geometry, and site effects. We have proposed a measure for quantitatively evaluating the appropriateness of synthesized time histories for engineering purposes, and have shown that based on this criterion, the method of Hutchings (1991) produces useful time histories.

Acknowledgments

We would like to thank Lawrence Hutchings for his invaluable suggestions and encouragement. Thanks also to Peter Goldstein for help with calculating the synthetic Green's functions and for many helpful discussions and reviews. Ralph Archuleta, John Anderson, Leif Wennerberg, Dave McCallen, Howard Patton, and an anonymous reviewer provided useful suggestions for improving the paper. We would also like to thank Elaine Price for reviewing the paper and providing helpful editorial comments. The LLNL Laboratory Directed Research and Development program provided funding for this project as part of the Computational Earthquake Hazards Initiative, and the LLNL Seismic Observatory provided computer support. The California Strong Motion Instrumentation Program, the U. S. Geological Survey, and Bechtel Corp. provided strong motion records. This work was performed under the auspices of the U. S. Department of Energy by the Lawrence Livermore National Laboratory under contract No. W-7405-ENG-48.

References

Abrahamson, N. A., P. G. Somerville, and C. A. Cornell (1990). Uncertainty in numerical strong motion predictions, Proc. Fourth U. S. Nat. Conf. on Earthquake Engineering vol. 1, 407–416.

Aki, K., and K. Irikura (1991). Characterization and mapping of earthquake shaking for seismic zonation, in *Proceedings of the Fourth International Conference on Seismic Zonation, Vol. I*, EERI, Oakland, 61-110.

Anderson, J. G. and G. Yu (1996). Predictability of strong motions from the Northridge, California earthquake, *Bull. Seism. Soc. Am.* **86**,???-???.

Archuleta, R. J., and S. Day (1980). Dynamic rupture in a layered medium: The 1966 Parkfield earthquake, *Bull. Seism. Soc. Am.* **70**, 671–690.

Bakun, W. H. (1984). Seismic moments, local magnitudes, and coda-duration magnitudes for earthquakes in central California, *Bull. Seism. Soc. Am*., **74**, 439–458.

Beroza, G.C. and P. Spudich (1988). Linearized inversion for fault rupture behavior: application to the 1984 Morgan Hill, California earthquake, *J. Geophys. Res.* **93**, 6275-6296.

Boatwright, J. (1988). The seismic radiation from composite models of faulting, *Bull. Seism. Soc. Am.* **78**, 489–508.

Bolt, B. A. (1992). Seismic strong motion synthetics, in Proceedings of the Caltrans Seismic Research Workshop.

Boore, D. M. (1983). Stochastic simulation of high-frequency ground motions, *Bull. Seism. Soc. Am*. **73**, 1865–1894.

Boore, D. M., Joyner, W. B., and T. E. Fumal (1993). Estimation of response spectra and peak accelerations from western North American earthquakes: an interim report, USGS Open File Report **93-509.**

Boore, D. M., L. Seekins, and W. B. Joyner (1989). Peak accelerations from the 17 October 1989 Loma Prieta earthquake, *Seism. Res. Lett.* **60**, 151-166

Carver, D., K. W. King, E. Cranswick, D. M. Worley, P. Spudich, and C. Mueller (1990). Digital recordings of aftershocks of the 17 October1989 Loma Prieta, California earthquake, Santa Cruz, Los Gatos, and surrounding areas, USGS Open File Report **90-683.**

Chin, B-H., and K. Aki (1991). Simultaneous study of the source, path, and site effects on strong ground motion during the 1989 Loma Prieta earthquake: a preliminary result on pervasive nonlinear site effects, *Bull. Seism. Soc. Am.* **81**, 1859–1884.

Cramer, C. H. (1995). Weak-motion observations and modeling for the Turkey Flat, U. S., site effects test area near Parkfield, California, *Bull. Seism. Soc. Am.* **85**, 440-451

Darragh, R. B, and A. F. Shakal (1991). The site response of two rock and soil station pairs to strong and weak ground motion, *Bull. Seism. Soc. Am.* **81**, 1885-1899.

Dietz, L. D., and W. L. Ellsworth (1990). The

October 17, 1989, Loma Prieta, California, earthquake and its aftershocks: geometry of the sequence from high-resolution locations, *Geophys. Res. Lett.* **17**, 1417–1420

Frankel, Arthur (1995). Simulating strong motion of large earthquakes using recordings of small earthquakes: the Loma Prieta main shock as a test case, *Bull. Seism. Soc. Am.* **85**, 1144-1160.

Freund, J. E. (1962). *Mathematical Statistics*, Prentice–Hall, Inc., Englewood Cliffs, N. J.

Field, E. H., and Jacob, K. H., (1993). Monte Carlo simulation of the theoretical site response variability at Turkey Flat, given uncertainty in the input parameters (abstract), *Seism. Res. Lett.* **64**, 17.

Hanks, T. C., and R. K. McGuire (1981). The character of high-frequency strong ground motion, *Bull. Seism. Soc. Am.* **71**, 2071–2095.

Hartzell, S.H. and T.H. Heaton (1988). Inversion of strong ground motion and teleseismic waveform data for the fault rupture history of the 1979 Imperial Valley, California, earthquake, B*ull. Seism. Soc. Am.* **73**, 1533-1583.

Hartzell, S. (1989).Comparison of seismic waveform inversion results for the rupture history of a finite fault: application to the 1986 North Palm Springs, California earthquake, *J. Geophys. Res.* **94** 7515-7534.

Hartzell, S. H., G. S. Stewart, and C. Mendoza (1991). Comparison of L_1 and L_2 norms in a teleseismic waveform inversion for the slip history of the Loma Prieta, California earthquake, *Bull. Seism. Soc. Am.* **81**, 1518–1539.

Hutchings, L. J. (1991). “Prediction” of strong ground motion for the 1989 Loma Prieta earthquake using empirical Green’s functions, *Bull. Seism. Soc. Am.* **81**, 1813–1837.

Hutchings, L. J. (1994). Earthquake models and synthesized ground motion for the 1971 San Fernando earthquake and aftershocks using empirical Green’s functions, *Bull. Seism. Soc. Am.* **84,** 1028-1050**.**

Hutchings, L. J., and F. Wu (1990). Empirical Green’s functions from small earthquakes: A waveform study of locally recorded aftershocks of the 1971 San Fernando earthquake, *J. Geophys. Res.* **95**, 1187–1214.

Hutchings, L. J., P. Goldstein, S. P. Jarpe, and P. W. Kasameyer (1992). Prediction of broadband near-field strong earthquake ground motion along an elongated structure from an extended fault rupture (abstract), *Seism. Res. Lett.* **63**, 31.

Irikura, K. (1983). Semi-empirical estimation of strong ground motions during large earthquakes. *Bull. Disaster Res. Inst*., Kyoto Univ., **33**, 63-104.

Iwan, W. D., M. A. Moser, and C-Y. Peng (1985). Some observations on strong motion earthquake measurement using a digital accelerograph, *Bull. Seism. Soc. Am*. **75**, 1225–1246.

Jarpe, S. P., L. J. Hutchings, T. F. Hauk, and A. F. Shakal (1989). Selected strong and weak motion data from the Loma Prieta earthquake sequence, *Seism. Res. Lett.* **60**, 167–176.

Joyner, W. B., and D. M. Boore (1981). Peak horizontal accelerations and velocity from strong motion records including records from the 1979 Imperial Valley, California, earthquake. *Bull. Seism. Soc. Am*., **71**, 2011–2038.

Joyner, W. B., and D. M. Boore (1986). On simulating large earthquakes by Green’s-function addition of smaller earthquakes, *Earthquake Source Mechanics*, Geophysical Monograph No. 37, Maurice Ewing, Ed., **8**, 269–274.

Joyner, W. B. and D. M. Boore (1988). Measurement characterization, and prediction of strong ground motion, in *Earthquake Engineering and Soil Dynamics II*, *Recent Advances in Ground-Motion Evaluatio*n, J. L. Von Thum (Editor), Geotechnical Special Publication No. 20, American Society of Civil Engineers, 43-102.

Kennedy, R. P., S. A. Short, K. L. Merz, F. J. Tokarz, I. M. Idriss, M. S. Power, and K. Sadigh (1984). *Engineering Characterization of Ground Motion-Task 1: Effects of Characteristics of Free-Field Response on Structural Response*, U. S. Nuclear Regulatory Commission NUREG/CR.

Kennett, B. L. N. (1983). *Seismic Wave Propagation in Stratified Media*, Cambridge University Press, Cambridge.

Maley, R., A. Acosta, F. Ellis, E. Etheredge, L. Foote, D. Johnson, R. Porcella, M. Salsman, and J. Switzer (1989). U. S. Geological Survey strong motion records from the Northern California (Loma Prieta) earthquake of October 17, 1989, U. S. Geological Surv. Open-File Rept. **89-568**.

McCallen, D. B., and K. M. Romstad (1994). Nonlinear model for building-soil systems, *J. Engrg. Mech., ASCE* **120**, 1129-1152.

McCallen, D.B. and L.J. Hutchings (1996). Ground motion estimation and nonlinear seismic analysis, proceedings: 12th Conference on Analysis and Computation of the American Society of Civil Engineers, Chicago, Illinois (in press).

Mueller, C., and G. Glassmoyer (1990). Digital recordings of aftershocks of the 17 October1989 Loma Prieta earthquake, USGS Open File Report **90-503.**

Munguia, L. and N. B. Brune (1984). Simulation of strong ground motion for earthquakes in the Mexicali-Imperial Valley region, *Geophys. J. Royal Astr. Soc.* **79**, 747–771.

Perez, V. (1973). Velocity response spectrum as a function of time, for the Pacoima Dam, San Fernando earthquake, February 9, 1971, *Bull. Seism. Soc. Am.*, **63**, 299-313.

Papageorgiou, A.S. and K. Aki (1983). A specific barrier model for the quantitative description of inhomogeneous faulting and the prediction of strong ground motion. I. Description of the model, *Bull. Seism. Soc. Am.* **73**, 693–722.

Popescu, R. and J. H. Prevost (1993). Numerical class ‘A’ predictions for model nos. 1, 2, 3, 4a, 4b, 6, 7, 11, and 12, in *Proc. International Conference VELACS 93*, A. A. Balkema, Ed., 1105-1129.

Schnabel, P. B., John Lysmer, and H. B. Seed (1973). SHAKE- a computer program for earthquake response analysis of horizontally layered sites, University of California, Berkeley Report EERC 72-12.

Schnabel, P. B. and H. B. Seed (1973). Accelerations in rock in the western United States, *Bull. Seism. Soc. Am.*, **63**, 501–516.

Shakal, A. F., M. Huang, M. Reichle, C. Ventura, T. Cao, R. Sherburne, M. Savage, R. Darragh, and C. Petersen (1989). CSMIP strong motion records from the Santa Cruz Mountains (Loma Prieta) earthquake of 17 October, 1989, CDMG SMIP Report OSMS **89-06**.

Snay, R. A., H. C. Neugebauer, and W. H. Prescott (1991). Horizontal deformation associated with the Loma Prieta earthquake, *Bull. Seism. Soc. Am.* **81**, 1647-1659.

Somerville, P., and J. Yoshimura (1990). The influence of critical Moho reflections on strong ground motion recorded in San Francisco and Oakland during the 1989 Loma Prieta earthquake, *Geophys. Res. Lett.* **17**, 1203–1206.

Somerville, P. (1993). Engineering applications of strong ground motion simulation, *Tectonophysics* **218**, 195–219.

Steidl, J. H., R. J. Archuleta, and S. H. Hartzell (1991). Rupture history of the Loma Prieta, California earthquake, *Bull. Seism. Soc. Am.* **81**, 1573–1602.

Trifunac, M. D. and A. G. Brady (1975a). On the correlation of peak accelerations of strong motions with earthquake magnitude, epicentral distance and site conditions, Proc U.S. National Conf. on Earthquake Eng., Ann Arbor, Michigan, 43–52.

Trifunac, M. D. and A. G. Brady (1975b). A study on the duration of strong earthquake ground motion, *Bull. Seism. Soc. Am.* **65,** 581-626.

Trifunac, M. D., and V. W. Lee (1985). Frequency dependent attenuation of strong earthquake ground motion., Department of Civil Engineering, University of Southern California, Report No. CE 85-02.

USGS (1990). Preliminary hypocentral locations from the Loma Prieta, California earthquake of October 17, 1989, U. S. Geol. Surv. Open-File Rept. **89-638**.

Wald, D. J., L. J. Burdick, and P. G. Somerville (1988). Simulation of acceleration time histories close to large earthquakes, *Earthquake*

*Engineering and Soil Dynamics II, Recent Advances in Ground-Motion Evaluatio*n, J.L. Von Thum (Editor), Geotechnical Special Publication No. 20, 430–444.

Wald, David J., Hiroo Kanamori, Donald V. Helmberger, and Thomas Heaton (1993). Source study of the 1906 San Francisco earthquake, *Bull. Seism. Soc. Am.* **83**, 981-1019.

Wald, D.J., D.V. Helmberger and S.H. Hartzell (1990). Rupture process of the 1987 Superstition Hills earthquake from inversion of strong-motion data, *Bull. Seism. Soc. Am.* **80**, 1079–1098.

Wald, D. J., T. H. Heaton, and K.W. Hudnut (1996) The slip history of the 1994 Northridge, California earthquake determined from strong - motion, teleseismic, GPS, and leveling data, *Bull. Seism. Soc. Am.* **86** ???-???.

Wallace, T. C., A. Velasco, J. Zhang, and T. Lay (1991). A broadband seismological investigation of the 1989 Loma Prieta, California earthquake: evidence for deep slow slip?, *Bull. Seism. Soc. Am.* **81**, 1622-1646.

Wennerberg, L. (1990). Stochastic summation of empirical Green's functions, *Bull. Seism. Soc. Am.* **80**, 1418–1432.

Wong, I. G., W. J. Silva, J. R. Humphrey, and I. P. Madin (1993). Site-specific ground motion estimates from a M_w 8.5 Cascadia Subduction Zone earthquake for the Portland, Oregon metropolitan area (abstract), *Seism. Res. Lett.* **64**, 17.

Zeng, Y., J. G. Anderson, and G. Yu (1994). A composite source model for computing realistic synthetic strong ground motions, *Geophys. Res. Lett.* **21**, 725-728.